



Left Ventricular Torsion in Hypertension and Hypertensive Heart Failure

— 3-Dimensional Speckle Tracking Echocardiography Assessment —

Shingo Minatoguchi, MD, PhD; Takashi Yoshizane, MD; Ryuhei Tanaka, MD, PhD;
Makoto Iwama, MD, PhD; Takatomo Watanabe, MD, PhD; Hidemaro Sato, BSc;
Maki Nagaya, BSc; Koji Ono, MD, PhD; Toshiyuki Noda, MD, PhD;
Sachiro Watanabe, MD, PhD; Shinya Minatoguchi, MD, PhD; Masanori Kawasaki, MD, PhD

Background: Left ventricular (LV) torsion by contraction of inner and outer oblique muscles contributes to EF. Outer muscle plays a predominant role in torsion. We evaluated the impact of LV remodeling by hypertension (HTN) on torsion using 3-dimensional speckle tracking echocardiography (3D-STE).

Methods and Results: LV strain, strain rate during systole (SR-S) and torsion at endocardium, mid-wall and epicardium were assessed on 3D-STE in 53 controls and 186 HTN patients. Torsion was defined as the difference between apical and basal rotation divided by long axis length. LVEF and strain, SR-S and torsion in all 3 layers in HTN without LV hypertrophy (LVH) were similar to those in controls. LV longitudinal strain at endocardium in HTN with LVH decreased, whereas LVEF was similar to that in controls and, which was associated with increased torsion at epicardium. Reduced LVEF in hypertensive HF was associated with reduced strain, SR-S and torsion in all layers and with LV dilation. On multivariate analysis, epicardial torsion was an independent determinant of LVEF. At epicardial torsion cut-off 0.41, the sensitivity and specificity for the identification of HF_{rEF} were 88% and 68%.

Conclusions: Torsion on 3D-STE may represent a compensatory mechanism to maintain LVEF despite reduced endocardial function, suggesting that the deterioration of torsion caused by insult to outer muscle and dilation may lead to HF_{rEF}.

Key Words: Left ventricular layer function; Left ventricular torsion; Speckle tracking echocardiography

The prevalence of heart failure (HF) increases with age, and hypertension (HTN), one of the most important risk factors for HF, also increases with age.^{1–3} The left ventricular (LV) wall thickness is increased in response to an elevated blood pressure as a compensatory mechanism to reduce the LV wall stress in HTN.^{3,4} LV torsion is increased in LV hypertrophy (LVH) with endocardial damage to preserve the LV ejection fraction (EF),⁵ whereas LV torsion will be reduced with increasing transmural damage, resulting in reduced EF. Alterations of the LV structure, function, and torsional deformation in the 3 myocardial layers associated with HTN, however, have not been fully examined on 3-dimensional speckle tracking echocardiography (3D-STE).^{2,6–9}

The orientation of myofibers changes across the LV wall: from a right-handed helix in the endocardium, circumferential orientation in the mid-wall to a left-handed helix in the epicardium.^{2,10} LV torsion caused by inner and

outer oblique muscle plays an important role in squeezing the blood out of the heart and may partly contribute to LVEF. Reduced endocardial function could result in reduced endocardial opposition to the dominant epicardium and, thus, enhanced torsion.² Therefore, LV remodeling such as hypertrophy, fibrosis and dilation caused by HTN may result in significant alterations of torsion. LV torsional deformation is a sensitive index of LV performance, and it therefore provides a useful index of myocardial mechanics, but is difficult to measure.¹¹ Using cardiac magnetic resonance (MR), it was reported that LV endocardial torsion is higher than epicardial torsion.¹²

The heart is a complex mechanical organ that undergoes cyclic changes in multiple dimensions.¹³ High-volume real-time 1-beat 3D-STE has enabled accurate evaluation of LV performance including the LV layer function assessed by strain and strain rate during systole (SR-S).^{6,14} Recently, STE has been validated as an accurate measurement of LV

Received January 7, 2019; revised manuscript received January 9, 2019; accepted January 10, 2019; J-STAGE Advance Publication released online February 2, 2019 Time for primary review: 1 day

Department of Cardiology, Gifu University Graduate School of Medicine, Gifu (Shingo M., T.W., Shinya M., M.K.); Department of Cardiology, Gifu Prefectural General Medical Center, Gifu (T.Y., M.I., M.N., K.O., T.N., S.W.); Department of Cardiology, Asahi University Hospital, Gifu (R.T.); and Department of Cardiology, Sawada Hospital, Gifu (H.S.), Japan

Mailing address: Shingo Minatoguchi, MD, PhD, Department of Cardiology, Gifu University Graduate School of Medicine, 1-1 Yanagido, Gifu 501-1194, Japan. E-mail: port735@gmail.com

ISSN-2434-0790 All rights are reserved to the Japanese Circulation Society. For permissions, please e-mail: cr@j-circ.or.jp

Variable	Control	Hypertension		HHF	
		LVH (-)	LVH (+)	HFpEF	HFrEF
n	53	50	61	32	43
Age (years)	67±10	68±11	70±11	79±12 ^{*,†‡}	68±16 [§]
Female	18 (34)	20 (40)	34 (56)	18 (56)	18 (42)
BSA (m ²)	1.63±0.20	1.64±0.21	1.63±0.24	1.52±0.20	1.66±0.23
SBP (mmHg)	124±13	133±16	137±14*	136±21*	135±29
DBP (mmHg)	71±10	74±10	75±12	72±17	77±21
HR (beats/min)	65±13	62±13	63±13	67±16	75±17 ^{*,†‡}
ACEI/ARB		33 (66)	40 (66)	25 (78)	32 (74)
β-blockers		12 (24)	11 (18)	20 (63)*	29 (67)*
Calcium antagonists		31 (62)	37 (61)	20 (63)	21 (49)
Diuretics		7 (14)	12 (20)	9 (28)	11 (26)
Statins	15 (28)	16 (32)	27 (44)	24 (75)	32 (74)

Data given as mean±SD or n (%). *P<0.05 vs. control, †P<0.05 vs. LVH (-), ‡P<0.05 vs. LVH (+), §P<0.05 vs. HFpEF. ACEI, angiotensin-converting enzyme inhibitor; ARB, angiotensin II receptor blocker; BSA, body surface area; DBP, diastolic blood pressure; HFpEF, heart failure with preserved ejection fraction; HFrEF, heart failure with reduced ejection fraction; HHF, hypertensive heart failure; HR, heart rate; LVH, left ventricular hypertrophy; SBP, systolic blood pressure.

rotation and torsion on comparison with sonomicrometry in dogs and MR in humans.^{15,16} The aims of the present study were therefore to evaluate the impact of LV remodeling caused by HTN on the LV layer function and torsion, and to elucidate the features of hypertensive HF (HHF) using 3D-STE.

Methods

Subjects and Study Protocol

Two hundred and fifty-eight patients with HTN who had systolic blood pressure (SBP) >140 mmHg or diastolic blood pressure >90 mmHg before treatment and who were treated with anti-hypertensive medication for >1 year, as well as 60 normotensive controls, were prospectively enrolled from January 2015 until April 2016. Hypertensive heart disease is defined as the presence of not only LVH but also complex changes in myocardial composition that are responsible for the structural and functional remodeling of myocardium in the absence of a cause other than HTN. The normotensive controls were recruited from subjects without HTN who were referred to hospital because of chest discomfort and who underwent electrocardiography and echocardiography without abnormal findings. Exclusion criteria were poor echocardiographic recording, presence of atrial fibrillation, moderate-severe valvular heart disease, past history of surgery for structural heart disease, cardiomyopathy and old myocardial infarction. Patients with coronary artery disease (CAD) proven on cardiac catheterization and diabetes mellitus were also excluded. Patients with HTN were divided into 4 groups according to the presence of LVH (LV mass index >115 g/m² in male patients and >95 g/m² in female patients)¹⁷ or HHF: HTN without LVH; HTN with LVH; HF with preserved EF (HFpEF); and HF with reduced EF (HFrEF). A diagnosis of HF was made according to the guidelines of the European Society of Cardiology.¹⁸ The HF group consisted of patients with both symptoms of HF (New York Heart Association class II or greater) and objective signs of HF, such as LVEF <50% or E/e' >15 or congestion and cardiomegaly on chest X-ray. The present study was

approved by the institution ethics committee, and all patients gave informed consent before participation (IRB number: G143).

LV Function and Structure on Conventional Echo-Doppler

A standard echo-Doppler examination was performed using a SC2000 ultrasound system (Siemens Medical Solutions, Mountain View, CA, USA) with a 4V1c transducer (1.25–4.5 MHz). Echocardiographic measurements were made according to the American Society of Echocardiography criteria.¹⁷ LVEF was measured using a biplane modified Simpson's method. The LV mass was calculated using the 2-D area-length method and indexed for body surface area (LVMI). Doppler measurements of mitral inflow E-wave and A-wave velocity were made from the apical 4-chamber view, and mitral annular tissue velocity during early filling (e') was measured at the septal mitral annulus to obtain E/e' as an index of LV filling pressure. The pulmonary capillary wedge pressure (PCWP) was estimated using the kinetics-tracking (KT) index, as previously reported.^{19,20} PCWP estimated by the KT index (ePCWP) and LV systolic stress were calculated using the following formulas:

$$ePCWP = 10.8 - 12.4 \times \log(\text{left atrial active emptying function/left atrial minimum volume index});^{19}$$

$$\text{LV systolic stress} = 0.334 \times \text{SBP} \times \text{LV end-systolic dimension} / \{ \text{LV end-systolic thickness} (1 + \text{LV end-systolic thickness/LV end-systolic dimension}) \} \text{ K dynes/cm}^2.^4$$

LV Performance on 3D-STE

We previously reported the feasibility of the novel high-volume 3D-STE for assessment of the LV layer function including LV strain and SR-S with good reproducibility.^{6,20} A full-volume scan can be acquired from only 1 heart beat with an apical approach using the SC2000 with the 4Z1c 3-D volumetric transducer. The recently developed software was applied to automatically divide the LV into 16 segments and calculate the LV strain, SR-S and torsion in the 3 layers with high volume rates.^{6,20}

LV contractility may be estimated with LV strain and

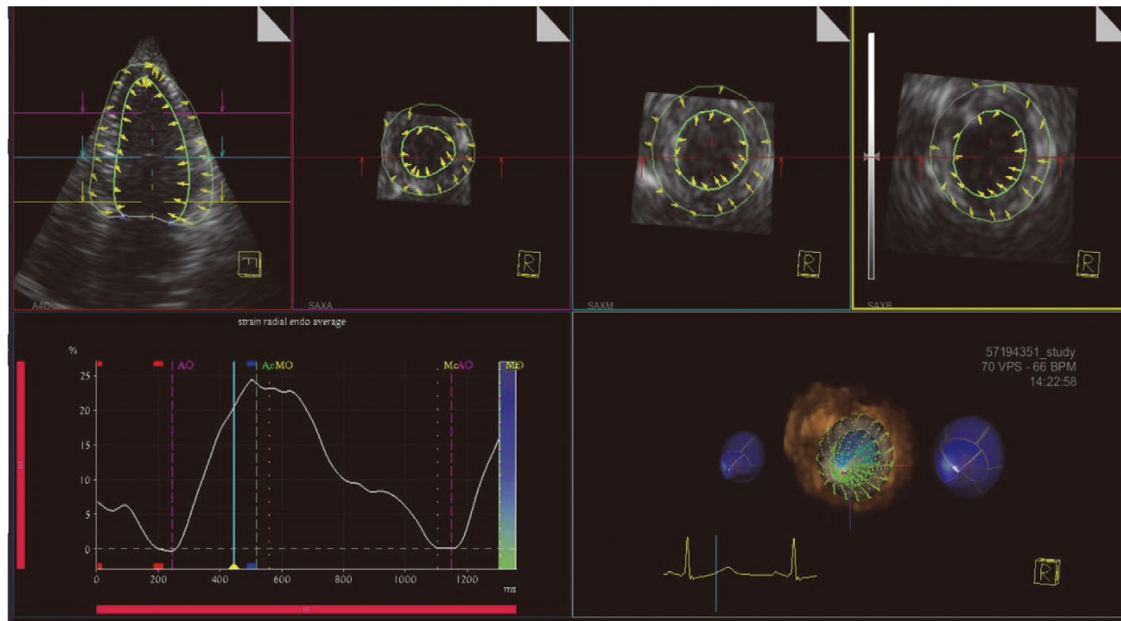


Figure 1. Full-volume acquisition and automated measurement of the left ventricle (LV) using high-volume 3-D speckle tracking echocardiography. (**Upper**) Automatic tracing of endocardial and epicardial borders of a 4-slice display for full-volume acquisition: 1 apical 4-chamber view and 3 short axis views. (**Lower left**) Time-strain curve obtained from the novel software at 70 vps; (**Lower right**) 3-D image of the LV. AO, aortic valve opening; MO, mitral valve opening.

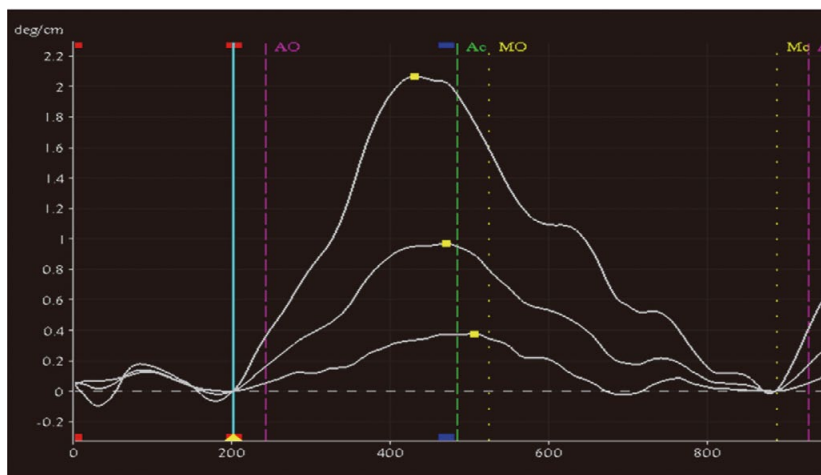


Figure 2. Time-left ventricular torsion curve at the (upper line) endocardium, (middle line) mid-wall, and (lower line) epicardium. AO, aortic valve opening; MO, mitral valve opening.

SR-S using tissue Doppler echocardiography imaging (TDI) and STE.^{13,21,22} We measured the LV strain in 3 directions and SR-S in the longitudinal and radial directions at the 3 layers as an index closely related to contractility. The time-LV torsion curve in the 3 myocardial layers is obtained using 3D-STE and the average of torsion of the 3 layers was used as global torsion. The ratio between LV global torsion and stroke volume (Torsion/SV) was calculated to estimate the effect of torsion compensation with LV volume change, a higher ratio of which represents a higher compensation of torsion for a lower SV.²³ The ratio between LV global torsion and LV strain (Torsion/strain)

was adopted to estimate torsion relative to myocardial dysfunction, with a higher ratio representing a higher degree of myocardial dysfunction.^{24,25}

Reliability and Reproducibility of LV Torsion on 3D-STE

We examined the interobserver variability of LV torsion measured on 3D-STE in 25 randomly selected recordings that were measured by 2 observers using 3D-STE in a blind manner. Similarly, we determined the intraobserver variability of torsion in 25 randomly selected recordings that were measured twice by 1 observer.

Variable	Control	Hypertension		HHF	
		LVH (-)	LVH (+)	HFpEF	HFrEF
LVEDD (mm)	28.7±3.3	28.0±4.5	29.8±6.0	29.4±5.1	45.5±10.3 ^{*,†,‡,§}
LVEDD (mm)	45.6±4.1	45.5±6.3	47.7±5.5	44.9±4.8	55.6±10.6 ^{*,†,‡,§}
LVTED (mm)	9.1±1.1	9.6±1.5	11.2±2.0 ^{*,†}	11.4±1.9 ^{*,†}	11.6±2.3 ^{*,†}
LVTES (mm)	13.6±2.1	13.4±2.3	14.8±2.9	15.1±2.6	14.8±2.4
3D-STE					
LVESV (mL)	37.8±12.0	37.8±18.7	45.8±20.9	46.2±20	108.6±47.8 ^{*,†,‡,§}
LVEDV (mL)	87.5±22.9	87.73±9.5	92.3±25.1	89.1±30.7	153.8±56.6 ^{*,†,‡,§}
SV (mL)	50.9±13.0	49.9±23.5	46.5±10.2	42.9±13.1	46.4±14.4
LV mass index (g/m ²)	90±18	93±19	130±32 ^{*,†}	128±37 ^{*,†,‡}	177±62 ^{*,†,‡,§}
LVEF (%)	67±6	68±5	68±7	64±9	37±9 ^{*,†,‡,§}
E/e'	9.3±2.7	11.0±3.3	12.1±5.2	16.9±8.3 ^{*,†,‡}	15.6±8.0 ^{*,†,‡,§}
ePCWP (mmHg)	7.4±2.9	7.6±4.6	9.0±4.3	14.7±4.5 ^{*,†,‡}	16.8±5.3 ^{*,†,‡}
Systolic stress (K dynes/cm ²)	62±19	65±22	65±27	62±23	107±40 ^{*,†,‡,§}

Data given as mean±SD. *P<0.05 vs. control, †P<0.05 vs. LVH (-), ‡P<0.05 vs. LVH (+), §P<0.05 vs. HFpEF. 3D-STE, 3-D speckle tracking echocardiography; E, early mitral inflow velocity; e', mitral annular early diastolic tissue velocity. ePCWP, estimated pulmonary capillary wedge pressure; HFpEF, heart failure with preserved ejection fraction; HFrEF, heart failure with reduced ejection fraction; HHF, hypertensive heart failure; LVEDD, left ventricular end-diastolic dimension; LVEDV, left ventricular end-diastolic volume; LVEF, left ventricular ejection fraction; LVESD, left ventricular end-systolic dimension; LVESV, left ventricular end-systolic volume; LVH, left ventricular hypertrophy; LVTED, left ventricular thickness at end-diastole; LVTES, left ventricular thickness at end-systole; SV, stroke volume.

Variable	Control	Hypertension		HHF	
		LVH (-)	LVH (+)	HFpEF	HFrEF
Radial strain					
Endocardium	35.7±8.1	36.1±8.4	33.0±8.6	30.4±11.3 ^{*,†}	20.0±6.1 ^{*,†,‡,§}
Mid-wall	34.6±7.9	35.1±8.1	31.7±8.2	29.7±10.5 ^{*,†}	20.0±6.1 ^{*,†,‡,§}
Epicardium	33.4±8.1	34.0±8.0	30.5±8.2	29.1±10.2 ^{*,†}	20.0±6.1 ^{*,†,‡,§}
Radial SR-S (/s)					
Endocardium	2.68±0.81	2.60±0.60	2.40±0.63	2.31±0.97 ^{*,†}	1.73±0.60 ^{*,†,‡,§}
Mid-wall	2.45±0.77	2.36±0.52	2.25±0.63	2.13±0.84 ^{*,†}	1.62±0.52 ^{*,†,‡,§}
Epicardium	2.15±0.63	2.09±0.46	2.03±0.52	1.84±0.70 ^{*,†}	1.52±0.48 ^{*,†,‡,§}
Longitudinal strain					
Endocardium	-19.2±3.2	-18.0±4.3	-16.0±4.5 [*]	-14.5±6.1 ^{*,†}	-10.5±4.2 ^{*,†,‡,§}
Mid-wall	-15.0±2.4	-13.9±3.0	-12.7±3.3	-11.3±4.4 ^{*,†}	-8.3±3.0 ^{*,†,‡,§}
Epicardium	-10.7±2.3	-9.7±2.2	-9.5±2.7	-8.1±3.2 ^{*,†}	-6.0±2.3 ^{*,†,‡,§}
Longitudinal SR-S (/s)					
Endocardium	-1.54±0.57	-1.44±0.36	-1.42±0.41	-1.27±0.74 ^{*,†}	-1.13±0.40 ^{*,†,‡,§}
Mid-wall	-0.84±0.30	-0.82±0.29	-0.78±0.29	-0.71±0.43 ^{*,†}	-0.67±0.28 ^{*,†,‡,§}
Epicardium	-0.46±0.19	-0.45±0.21	-0.44±0.17	-0.36±0.25	-0.36±0.18 ^{*,†,‡,§}
Circumferential strain					
Endocardium	-29.3±5.6	-29.5±8.2	-26.4±6.4	-24.8±5.1	-15.5±5.3 ^{*,†,‡,§}
Mid-wall	-19.4±3.9	-19.6±5.2	-18.0±4.2	-16.9±3.7	-10.7±3.4 ^{*,†,‡,§}
Epicardium	-9.5±3.6	-9.8±3.1	-9.7±3.0	-9.0±3.0	-5.9±2.8 ^{*,†,‡,§}
Torsion (°/cm)					
Endocardium	2.48±0.34	2.44±0.42	2.32±0.30	2.19±0.49 ^{*,†}	1.91±0.31 ^{*,†,‡,§}
Mid-wall	1.18±0.22	1.25±0.30	1.32±0.31	1.21±0.31	0.98±0.20 ^{*,†,‡,§}
Epicardium	0.48±0.22	0.55±0.28	0.64±0.26 [*]	0.56±0.30	0.33±0.15 ^{*,†,‡,§}
Global torsion (°/cm)					
Global twist (°)	1.38±0.20	1.43±0.30	1.50±0.31	1.33±0.31	1.04±0.17 ^{*,†,‡,§}
Torsion/longitudinal strain					
Torsion/SV	0.029±0.008	0.034±0.016	0.034±0.012	0.036±0.015 [*]	0.025±0.009 ^{*,†,‡,§}
Torsion at epicardium/SV					
Torsion at epicardium/SV	0.010±0.006	0.013±0.009	0.014±0.007 [*]	0.015±0.008 [*]	0.008±0.004 ^{*,†,‡,§}

Data given as mean±SD. *P<0.05 vs. control, †P<0.05 vs. LVH (-), ‡P<0.05 vs. LVH (+), §P<0.05 vs. HFpEF. LV, left ventricular; SR-S, strain rate during systole. Other abbreviations as in Table 2.

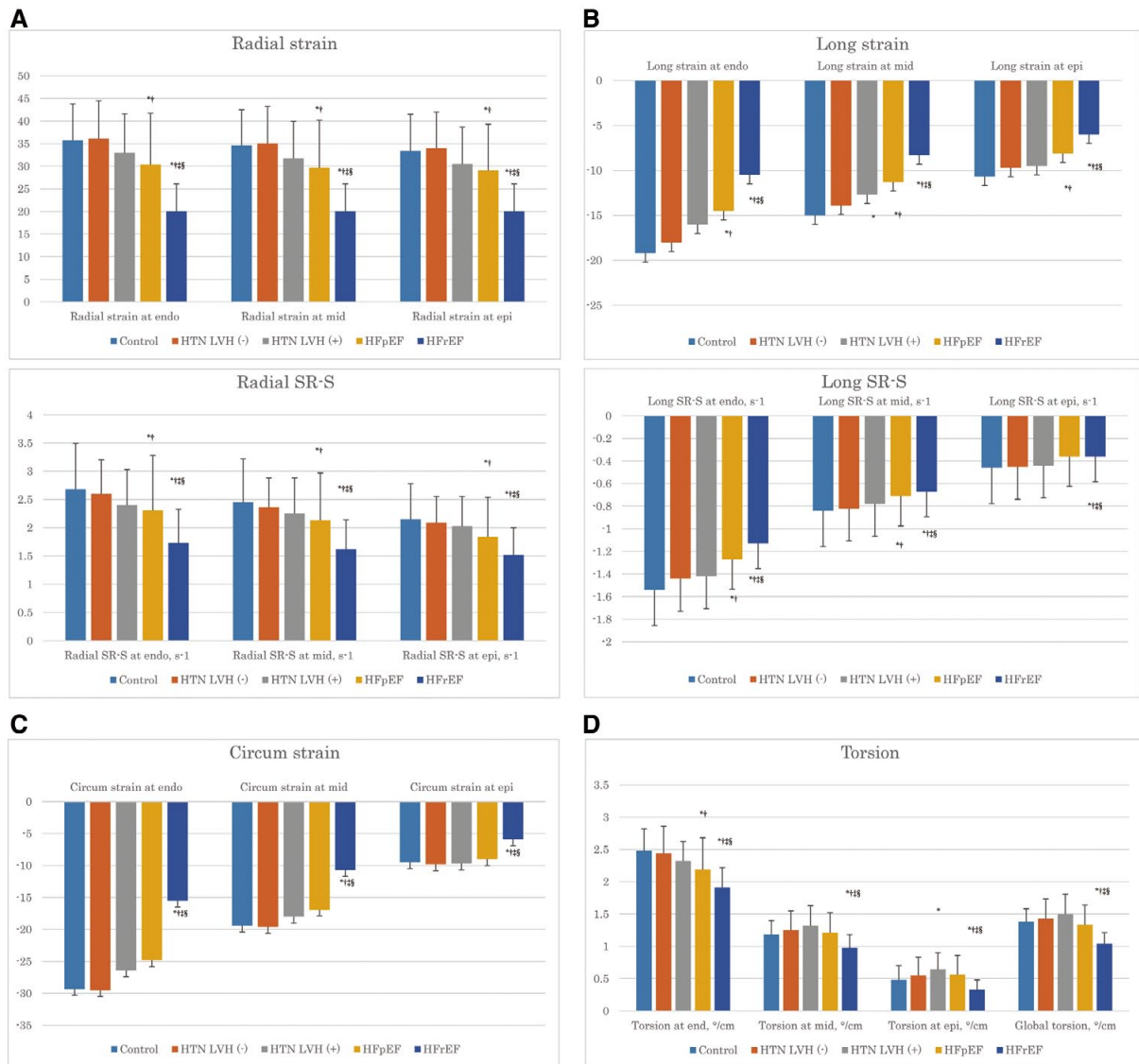


Figure 3. Left ventricular (LV) deformation parameters at endocardium (endo), mid-wall (mid) and epicardium (epi) in controls, patients with hypertension (HTN) with or without LV hypertrophy (LVH), and patients with heart failure with preserved ejection fraction (HFpEF) and heart failure with reduced ejection fraction (HFrEF): **(A)** radial strain and strain rate during systole (SR-S); **(B)** longitudinal strain and SR-S; **(C)** circumferential strain; and **(D)** LV torsion. * $P < 0.05$ vs. control, † $P < 0.05$ vs. HTN LVH (-), ‡ $P < 0.05$ vs. HTN LVH (+), § $P < 0.05$ vs. HFpEF.

Statistical Analysis

Continuous variables are expressed as mean \pm SD, and categorical variables as frequency and percentage. Differences between groups for the categorical variables were assessed using chi-squared test or Fisher's exact test, and differences between groups for the continuous variables were assessed using analysis of variance followed by Bonferroni test for post-hoc comparisons. Multivariate logistic analysis was performed to determine the independent features of HFpEF and HFrEF in the HTN groups because HTN is a major risk factor of HF. Receiver operating characteristic (ROC) curve analysis was used to discriminate patients with HFpEF and HFrEF based on the parameters derived using 3D-STE, and we determined

the sensitivity, specificity, positive and negative predictive values (PPV and NPV) and area under the curve (AUC). $P < 0.05$ was considered significant. All analyses were performed using SPSS version 21.0 (IBM).

Results

Subjects

We enrolled 273 patients with HTN and 60 normotensive controls. Patients with poor echocardiographic recording ($n=8$), atrial fibrillation including 15 patients with HFpEF ($n=27$), valvular heart disease ($n=13$), past history of cardiac surgery ($n=6$), cardiomyopathy ($n=6$), myocardial infarction ($n=10$), CAD ($n=8$) and diabetes mellitus ($n=16$) were

Table 4. Multivariate Indicators of HFpEF and HFrEF

Category	β	SE	Wald	OR	95%CI		P-value
					Lower	Upper	
A. HFpEF (n=143)*							
Torsion at endocardium	-1.435	0.627	5.231	0.238	0.070	0.814	0.022
ePCWP	0.259	0.057	20.478	1.295	1.158	1.449	<0.001
Age	0.091	0.028	10.353	1.095	1.036	1.157	0.001
B. HFrEF (n=186)†							
E/e'	-0.1199	0.0612	3.8431	0.8870	0.7868	1.0000	0.0499
Longitudinal strain at epicardium	0.6695	0.1810	13.6853	1.9533	1.3700	2.7850	0.0002
Torsion at endocardium	-1.4758	0.8882	2.7609	0.2286	0.0401	1.3034	0.0966
Torsion at epicardium	-7.2277	2.6269	7.5705	0.0007	0.0000	0.1250	0.0059
ePCWP	0.2741	0.0757	13.0956	1.3153	1.1339	1.5258	0.0003
Systolic stress	0.0313	0.0099	9.8717	1.0318	1.0118	1.0521	0.0017

*Hypertension and HFpEF; †hypertension and HFrEF. SE, standard error. Other abbreviations as in Table 2.

Table 5. Prediction Ability of HF Features

Category	AUC	P-value	Cut-off	Sensitivity	Specificity	PPV	NPV
A. Features of HFpEF (n=143)*							
Torsion at endocardium (°/cm)	0.68	0.002	2.11	69	75	44	89
Age (years)	0.76	<0.001	74.5	69	70	40	89
ePCWP (mmHg)	0.85	<0.001	11.02	78	76	48	92
B. Echocardiography features of HFrEF (n=186)†							
E/e'	0.622	0.016	12.2	63	62	33	85
Longitudinal strain at epicardium	0.872	<0.001	-7.3	79	80	54	93
ePCWP (mmHg)	0.836	<0.001	12.1	84	73	48	94
Systolic stress (K dynes/cm ²)	0.838	<0.001	86.1	72	89	66	91
Torsion at epicardium (°/cm)	0.805	<0.001	0.41	88	68	45	95
Global Torsion (°/cm)	0.874	<0.001	1.15	70	86	60	90

*Hypertension and HFpEF; †hypertension and HFrEF. AUC, area under the curve; NPV, negative predictive value; PPV, positive predictive value. Other abbreviations as in Table 2.

excluded. Accordingly, 186 patients with HTN (50 patients without LVH, 61 patients with LVH [44 patients with concentric LVH and 17 patients with eccentric LVH], 32 patients with HFpEF and 43 patients with HFrEF) and 53 controls were finally enrolled. Patient characteristics are listed in **Table 1**.

Reproducibility of LV Torsion on Novel 3D-STE

The intraobserver correlation coefficient and variability in LV global torsion measured using the novel 3D-STE were 0.96 and 0.0±7.0%, respectively. The interobserver correlation coefficient and variability in LV global torsion using the novel 3D-STE were 0.95 and 0.5±7.2%, respectively.

Echocardiography Parameters

LV layer strain, SR-S and torsion were obtained in ≤3 min (145±10s) using 3D-STE at a volume rate of 69±6 vps (range, 59–86 vps) and the novel software (**Figures 1,2**). Data from standard and conventional echo-Doppler and LV deformational parameters assessed on 3D-STE are given in **Tables 2,3**. LV strain, SR-S and torsion are shown in **Figure 3**. LVEF, strain, SR-S and torsion in all 3 layers in HTN without LVH were similar to those of controls. The LV longitudinal strain at the endocardium was reduced in HTN with LVH, whereas LVEF was similar to that of controls which are related with increased torsion at

the epicardium. LVEF in HFpEF was also preserved in association with a preserved global torsion and increased Torsion/SV despite decreased strain in all 3 layers in the radial and longitudinal directions, and a decrease in all SR-S except longitudinal SR-S at the epicardium. LVEF in HFrEF was the most markedly decreased of the 5 groups, associated with not only a reduced LV strain and SR-S in all 3 layers, but also a reduced torsion in all 3 layers. Patients with HFrEF had a significantly larger LV end-diastolic diameter than others, and larger diameter was associated with reduced torsion ($r=-0.39$, $P<0.01$). In contrast, LV global twist was not decreased in HFrEF. The amplitudes of peak torsion at the epicardium and global torsion in the total subjects were correlated with LVEF (epicardium, $r=0.33$; global torsion, $r=0.50$; both $P<0.001$). Peak torsion at the endocardium in the controls was significantly greater than the corresponding torsion at the mid-wall and epicardium by 52% and 80%, respectively. The decreasing LV layer torsion from endocardium to epicardium was observed in all groups. LV epicardial torsion/SV increased in HTN with LVH and HFpEF, whereas that and global torsion/SV decreased in HFrEF. LV global torsion/longitudinal strain was the largest in HFrEF of the 5 groups.

Independent Features of HFpEF and HFrEF on Echocardiography

Multivariate logistic analysis was performed to determine the independent echocardiographic variables associated with HFpEF and HFrEF, but parameters showing strong multicollinearity were excluded. ePCWP showed a stronger association with HFpEF (Table 4A). Using 11.02 mmHg as an optimal cut-off from ROC curve analysis, the sensitivity and specificity for HFpEF were 78% and 76%, respectively, and the PPV and NPV were 48% and 92%, respectively, with an AUC of 0.85 (Table 5A). LV epicardial torsion showed a stronger association with HFrEF (Table 4B). Using 0.41°/cm as an optimal cut-off from ROC curve analysis, the sensitivity and specificity for HFrEF were 88% and 68%, respectively, and the PPV and NPV were 45% and 95%, respectively, with an AUC of 0.81 (Table 5B). Furthermore, using a global torsion cut-off of 1.15 from ROC curve analysis, the sensitivity and specificity for HFrEF were 70% and 86%, respectively, and the PPV and NPV were 60% and 90%, respectively, with an AUC of 0.87 (Table 5B).

Discussion

This is the first study to examine LV layer torsion in HTN and HHF using high-volume real-time 1-beat 3D-STE. We showed that LVEF in HTN with LVH was preserved, accompanied with increased torsion at the epicardium despite decreased longitudinal strain at the endocardium, and that LVEF in HFpEF was also preserved, in association with preserved global torsion and increased torsion/SV despite a decreased LV strain and SR-S. We also demonstrated that the LV layer torsion and global torsion in HFrEF were all decreased in association with reduced strain and SR-S in the 3 layers in all directions, and with LV dilation. This suggested that LV remodeling in HTN with LVH and HFpEF could cause a myocardial insult in an endocardial layer, resulting in reduced endocardial function and relatively enhanced outer oblique muscle function and epicardial torsion to preserve LVEF as a compensatory mechanism. When myocardial insult caused by HTN progresses through the entire myocardial layer, LV epicardial function becomes impaired, accompanied by LV dilation and reduced torsion, which may lead to HFrEF.

LV Myocardial Layers and LV Torsion

The LV is composed of 3 myocardial layers and the orientation of myofibers gradually changes across the LV wall.^{2,10,26} Chitiboi et al examined LV layer torsion using MR, and found that LV torsion at the endocardium is higher than that at the epicardium.¹² It is useful to know the cardiac micro- and macro-architectures in order to understand the relative contributions of different myocardial layers to the 3-D components of myocardial deformation and torsion.²⁷ The subendocardial fibers may be more susceptible to dysfunction than the mid- and epicardial fibers.²⁸ This impairment of the subendocardial fibers also leads to attenuated subendocardial right-handed helix fiber shortening during systole, potentially resulting in a failure to fully counterbalance the subepicardial left-handed helix fiber shortening, and resulting in increased circumferential deformation and torsional deformation as well.^{29,30}

LV torsion plays an important role in squeezing the blood out of the heart and may partly contribute to EF with a more efficient contraction.^{31,32} Although the amplitude

of peak rotation in the epicardium is lower than that in the endocardium, the LV outer oblique muscle plays a predominant role in LV torsion,¹⁰ because the outer oblique muscle is at a greater radius from the LV central long axis and thus has longer arms than the inner muscle to produce a greater moment. Moreover, the epicardium contains more fibers in a given epicardial volume shell than an endocardial volume shell of the same thickness. Therefore, global LV torsional deformation appears to be controlled by the epicardial myocardium. Furthermore, LV dilation is associated with stretching and reorientation of the muscle bundles in such a manner that the relative angle between the main fiber bundles is reduced, with fibers in both layers coursing more circumferentially, resulting in reduction of torsion.

Therefore, insult to the endocardium by HTN enhances the LV epicardial function, resulting in increased epicardial torsion, as we demonstrated.

Utility of 3-D Strain Echocardiography in LV Torsion Assessment

The heart is a complex mechanical organ that undergoes cyclic changes in multiple dimensions that ultimately effect a change in the chamber volume, function and deformation.¹³ LV deformation is characterized by torsion as well as longitudinal, radial and circumferential motion. Although myocardial deformation in 3 directions can be quantified and LV twist can be measured on 2D-STE, which was validated against sonomicrometry and tagged MR,⁷⁻⁹ assessment of LV torsion as an index of LV deformation in 4 dimensions on echocardiography has been methodologically challenging, because real-time 1-beat 3D-STE is an emerging technology, and the distance between the basal and apical short axis slices is difficult to accurately assess simultaneously with measurement of the basal and apical rotation using conventional echocardiography.² Although 3D-STE could eliminate the confounding effects of through-plane myocardial motion, the lower temporal and spatial resolution of low-volume 3D-STE could adversely affect the accuracy of 3D-STE measurement. In contrast, high-volume real-time 1-beat 3D-STE enables more accurate evaluation of the torsion and SR without stitching image, and measurement of the peak of those indexes because of the higher temporal and spatial resolution. Thus, the complex mechanics of LV torsion may be best represented by high-volume novel real-time 1-beat 3-D strain echocardiography.

LV Torsion in HTN and HHF

HTN can lead to LV macro- and microvascular abnormalities and interstitial fibrosis.³³ Given that the endocardium is the most susceptible to the deleterious effects of interstitial fibrosis and hypoperfusion, endocardial function can deteriorate at an earlier stage.³² In the present study, LV torsion of the 3 layers was the smallest in HFrEF of the 5 groups. Yoneyama et al reported that given that the oblique fiber structure of the endocardium and epicardium is oriented in different directions, a reduced endocardial function may alter the balance between opposing rotational forces and, thus, result in enhanced torsion on MR.² We showed that LV epicardial torsion in HTN with LVH increased in association with a reduced endocardial function and that LV torsion in all layers in HFrEF decreased in association with reduced LV strain and SR-S at the epicardium, as well as at the endocardium and mid-wall on

3D-STE. This may indicate that LV layer remodeling alters the balance of rotational forces and influences LV layer torsion. Therefore, the present study suggests that LV torsion is an important indicator of cardiac performance, reflected by the layer function, and that LVH, fibrosis and dilation caused by HTN could result in significant alterations of torsion.

Wang et al reported that LV twist reduced in patients with systolic HF associated with a reduced longitudinal, radial and circumferential strain, but that twist was not reduced in patients with diastolic HF accompanied with preserved circumferential strain.³⁴ In contrast, in the present study the LV twist in HFrEF was similar to that in the controls, and twist in HTN with LVH was the highest in the 5 groups. This suggests that normalized torsion may more accurately reflect the LV layer function and LV performance than twist. Therefore, LV torsion may reflect LV structural as well as functional remodeling.

A transmural insult or progression of disease results in concomitant mid-wall and epicardial dysfunction, leading to reductions in LV torsion mechanics and LVEF.³⁵ In the present study, Torsion/SV in HFpEF was increased compared with the control, and that in HFrEF was decreased compared with HTN with or without LVH and HFpEF, suggesting that compensation for torsion might be impaired in HFrEF. Furthermore, Torsion/SV in HFrEF was low regardless of having the same SV as that in HFpEF, which shows that the preserved SV in HFrEF in the present study was thought to be due not to LV torsion but to LV dilation (large LV end-diastolic volume).

Torsion/strain was the highest in HFrEF of the 5 groups, suggesting a higher degree of LV dysfunction in HFrEF. On multivariate logistic analysis, reduced epicardial torsion and reduced longitudinal strain at the epicardium are independent features of HFrEF in HTN groups. Thus, understanding the layer-based contributions to the components of cardiac deformation, especially torsion, helps in correctly estimating the transmural disease burden due to HTN and provides pathophysiologic insight into the mechanisms of LV dysfunction.

Study Limitations

There are several limitations in the present study. First, we could not validate the values of torsion obtained on real-time 1-beat 3D-STE using MR as a reference standard. Although validation of 3D-STE on assessment of the LV function and rotation has been performed in animal studies using sonomicrometry as the reference standard,³⁶ and validation of the value of torsion derived from 2D-STE has been performed in humans using MR,³⁷ several studies still examined LV torsion using STE without validation.³⁵ Of course, further validation studies of this novel 3D-STE against highly accurate references are needed. Second, the number of patients with HFpEF and HFrEF was small. LV twist has been reported to be preserved or increased in HFpEF, and reduced in HFrEF,^{34,38} whereas, in the present study, LV torsion but not twist was reduced in HFrEF. Thus, further studies with larger patient groups including HFrEF and HFpEF are needed. Finally, we cannot deny the possibility that we enrolled patients with cardiomyopathy complicated with HTN as HFrEF.

Conclusion

LV torsion may represent a compensatory mechanism to

maintain an adequate stroke volume and LVEF despite reduced systolic function at the endocardium by the relative enhancement of torsion at the epicardium. Deterioration of LV torsion, which reflects an insult to the total layer, including the outer oblique muscle, could lead to HFrEF with LV dilation. LV torsion may reflect LV structural and functional remodeling, and the assessment of LV torsion on 3D-STE may be useful to understand the mechanism of LV systolic performance and to detect LV layer insult in HTN and HFrEF.

Disclosures

The authors declare no conflicts of interest.

References

- Ceia F, Fonseca C, Mota T, Morais F, de Sousa A, Oliveira A. Prevalence of chronic heart failure in southwestern Europe: The EPICA study. *Eur J Heart Fail* 2002; **4**: 531–539.
- Yoneyama K, Gjesdal O, Choi EU, Wu CO, Hundley WG, Gomes AS, et al. Age, gender and hypertension-related remodeling influences left ventricular torsion assessed by tagged cardiac magnetic resonance in asymptomatic individuals: The Multi-ethnic study of atherosclerosis. *Circulation* 2012; **126**: 2481–2490.
- Drazner MH. The progression of hypertensive heart disease. *Circulation* 2011; **123**: 327–334.
- Grossman W, Jones D, McLaurin LP. Wall stress and patterns of hypertrophy in the human left ventricle. *J Clin Invest* 1975; **56**: 56–64.
- Yoneyama K, Donekal S, Venkatesh BA, Wu CO, Liu CY, Nacif MS, et al. Natural history of myocardial function in an adult human population: Serial longitudinal observations from MESA. *J Am Coll Cardiol Cardiovasc Imaging* 2016; **9**: 1164–1173.
- Saeki M, Sato N, Kawasaki M, Tanaka R, Nagaya M, Watanabe T, et al. Left ventricular layer function in hypertension assessed by myocardial strain rate using novel one-beat real-time three-dimensional speckle tracking echocardiography with high volume rates. *Hypertens Res* 2015; **38**: 551–559.
- Goffinet C, Chenot F, Robert A, Pouleur AC, le Polain de Waroux JB, Vanvraynest D, et al. Assessment of subendocardial vs. subepicardial left ventricular rotation and twist using two-dimensional speckle tracking echocardiography: Comparison with tagged cardiac magnetic resonance. *Eur Heart J* 2009; **30**: 608–617.
- Marcus KA, Mavinkurve-Groothuis AM, Barends M, van Dijk A, Feuth T, de Korte C, et al. Reference values for myocardial two-dimensional strain echocardiography in a healthy pediatric and young adult cohort. *J Am Soc Echocardiogr* 2011; **24**: 625–636.
- Amundsen BH, Helle-Valle T, Edvardsen T, Torp H, Crosby J, Lyseggen E, et al. Noninvasive myocardial strain measurement by speckle tracking echocardiography: Validation against sonomicrometry and tagged magnetic resonance imaging. *J Am Coll Cardiol* 2006; **47**: 789–793.
- Streeter DD Jr, Spotnitz HM, Patel DP, Ross J Jr, Sonnenblick EH. Fiber orientation in the canine left ventricle during diastole and systole. *Circ Res* 1969; **24**: 339–347.
- Notomi Y, Setser RM, Shiota T, Martin-Miklovic MG, Weaver JA, Popovic ZB, et al. Assessment of ventricular torsional deformation by Doppler tissue imaging. *Circulation* 2005; **111**: 1141–1147.
- Chitiboi T, Schnell S, Collins J, Carr J, Chowdhary V, Honarmand AR, et al. Analyzing myocardial torsion based on tissue phase mapping cardiovascular magnetic resonance. *J Cardiovasc Magn Reson* 2016; **18**: 15.
- Abraham TP, Dimaano VL, Liang HY. Role of tissue Doppler and strain echocardiography in current clinical practice. *Circulation* 2007; **116**: 2597–2609.
- Minatoguchi S, Kawasaki M, Tanaka R, Yoshizane T, Ono K, Saeki M, et al. Evaluation of systolic and diastolic properties of hypertensive heart failure using speckle tracking echocardiography with high volume rates. *Heart Vessels* 2017; **32**: 1202–1213.
- Helle-Valle T, Crosby J, Edvardsen T, Lyseggen E, Amundsen BH, Smith HJ, et al. New noninvasive method for assessment of left ventricular rotation; speckle tracking echocardiography. *Circulation* 2005; **112**: 3149–3156.

16. Lamia B, Tanabe M, Tanaka H, Kim HK, Gorcsan J 3rd, Pinsky MR. Left ventricular systolic torsion correlates global cardiac performance during dyssynchrony and cardiac resynchronization therapy. *Am J Physiol Heart Circ Physiol* 2011; **300**: H853–H858.
17. Lang RM, Bierig M, Devereux RB, Flachskampf FA, Foster E, Pellikka PA, et al. Recommendations for chamber quantification: A report from the American Society of Echocardiography's Guidelines and Standard Committee and the Chamber Quantification Writing Group, developed in conjunction with the European Association of Echocardiography. *J Am Soc Echocardiogr* 2005; **18**: 1440–1463.
18. Swedberg K, Cleland J, Dargie H, Drexler H, Follath F, Komajda M, et al. Guidelines for the diagnosis and treatment of chronic heart failure. *Eur Heart J* 2005; **26**: 1115–1140.
19. Kawasaki M, Tanaka R, Ono K, Minatoguchi S, Watanabe T, Iwama M, et al. A novel ultrasound predictor of pulmonary capillary wedge pressure assessed by the combination of left atrial volume and function: A speckle tracking echocardiography study. *J Cardiol* 2015; **66**: 253–262.
20. Kawasaki M, Tanaka R, Yoshida A, Nagaya M, Minatoguchi S, Yoshizane T, et al. Non-invasive pulmonary capillary wedge pressure assessment on speckle tracking echocardiography as a predictor of new-onset non-valvular atrial fibrillation. *Circ J* 2018; **82**: 3029–3036.
21. Hoit BD. Strain and strain rate echocardiography and coronary artery disease. *Circ Cardiovasc Imaging* 2011; **4**: 179–190.
22. Kovacs A, Olash A, Lux A, Matyas C, Nemeth BT, Kellermayer D, et al. Strain and strain rate by speckle tracking echocardiography correlate with pressure-volume loop derived contractility indices in a rat model of athlete's heart. *Am J Physiol Heart Circ Physiol* 2015; **308**: H743–H748.
23. Notomi Y, Popovic ZB, Yamada H, Wallick DW, Martin MG, Oryszak SJ, et al. Ventricular untwisting: A temporal link between left ventricular relaxation and suction. *Am J Physiol Heart Circ Physiol* 2008; **294**: H505–H513.
24. Lumens J, Delhaas T, Arts T, Cowan BR, Young AA. Impaired subendocardial contractile myofiber function in asymptomatic aged humans, as detected using MRI. *Am J Physiol Heart Circ Physiol* 2006; **291**: H1573–H1579.
25. Van Der Toorn A, Barenbrug P, Snoep G, Van Der Veen FH, Delhaas T, Prinzen FW, et al. Transmural gradients of cardiac myofiber shortening in aortic valve stenosis patients using MRI tagging. *Am J Physiol Heart Circ Physiol* 2002; **283**: H1609–H1615.
26. Covell JW. Tissue structure and ventricular wall mechanics. *Circulation* 2008; **118**: 699–701.
27. Mor-Avi V, Lang RM, Badano L, Belohlavek M, Cardim NM, Derumeaux G, et al. Current and evolving echocardiographic techniques for the quantitative evaluation of cardiac mechanics: ASE/EAE consensus statement on methodology and indications endorsed by the Japanese Society of Echocardiography. *J Am Soc Echocardiogr* 2011; **24**: 277–313.
28. Biering-Sørensen T, Hoffmann S, Mogelvang R, Zeeberg Iversen A, Galatius S, Fritz-Hansen T, et al. Myocardial strain analysis by 2-dimensional speckle tracking echocardiography improves diagnostics of coronary artery stenosis in stable angina pectoris. *Circ Cardiovasc Imaging* 2014; **7**: 58–65.
29. Kraigher-Krainer E, Shah AM, Gupta DK, Santos A, Claggett B, Pieske B, et al; PARAMOUNT Investigators. Impaired systolic function by strain imaging in heart failure with preserved ejection fraction. *J Am Coll Cardiol* 2014; **63**: 447–456.
30. Biering-Sørensen T, Solomon SD. Assessing contractile function when ejection fraction is normal: A case for strain imaging. *Circ Cardiovasc Imaging* 2015; **8**: e004181.
31. Ingels NB Jr, Hansen DE, Daughters GT 2nd, Stinson EB, Alderman EL, Miller DC. Relation between longitudinal, circumferential, and oblique shortening and torsional deformation in the left ventricle of the transplanted human heart. *Circ Res* 1989; **64**: 915–927.
32. Lumens J, Delhaas T, Arts T, Cowan BR, Young AA. Impaired subendocardial contractile myofiber function in asymptomatic aged humans, as detected using MRI. *Am J Physiol Heart Circ Physiol* 2006; **291**: H1573–H1579.
33. Martinez DA, Guhl DJ, Stanley WC, Vailas AC. Extracellular matrix maturation in the left ventricle of normal and diabetic swine. *Diabetes Res Clin Pract* 2003; **59**: 1–9.
34. Wang J, Khoury DS, Yue Y, Torre-Amione G, Nagueh SF. Preserved left ventricular twist and circumferential deformation, but depressed longitudinal and radial deformation in patients with diastolic heart failure. *Eur Heart J* 2008; **29**: 1283–1289.
35. Bansal M, Leano RL, Marwick TH. Clinical assessment of left ventricular systolic torsion: Effects of myocardial infarction and ischemia. *J Am Soc Echocardiogr* 2008; **21**: 887–894.
36. Seo Y, Ishizu T, Enomoto Y, Sugimori H, Aonuma K. Endocardial surface area tracking for assessment of regional LV wall deformation with 3D speckle tracking imaging. *J Am Coll Cardiol Cardiovasc Imaging* 2011; **4**: 358–365.
37. Notomi Y, Lysyansky P, Setser RM, Shiota T, Popovic ZB, Martin-Miklovic MG, et al. Measurement of ventricular torsion by two-dimensional ultrasound speckle tracking imaging. *J Am Coll Cardiol* 2005; **45**: 2034–2041.
38. Omar AM, Vallabhajosyula S, Sengupta PP. Left ventricular twist and torsion: Research observations and clinical applications. *Circ Cardiovasc Imaging* 2015; **8**: pii: e003029.